iJRASET
International Journal For Research in Applied Science and Engineering Technology

INTERNATIONAL JOURNAL FOR RESEARCH

IN APPLIED SCIENCE & ENGINEERING TECHNOLOGY

Volume: 14 **Issue:** VI **Month of publication:** June 2026

DOI: https://doi.org/10.22214/ijraset.2026.83506

www.ijraset.com

Call: 08813907089 | E-mail ID: ijraset@gmail.com

International Journal for Research in Applied Science & Engineering Technology (IJRASET)
ISSN: 2321-9653; IC Value: 45.98; SJ Impact Factor: 7.538
Volume 14 Issue VI June 2026- Available at www.ijraset.com

Hierarchical Battery Pack Integration and Parametric Analysis for eBAJA Electric All-Terrain Vehicle Powertrain Simulation in MATLAB/Simulink

Mrunal Dhawade[1], Parth Dhage[2]
K. J. College of Engineering and Management Research, Pune, India

Abstract: ***This paper presents the design, implementation, and parametric analysis of a hierarchical battery pack integration for the eBAJA electric all-terrain vehicle (eATV) powertrain simulation in MATLAB/Simulink. Working from the MathWorks eBAJA reference model, the lumped equivalent circuit model (ECM) battery is replaced with a hierarchical Battery Builder pack comprising five series-connected module assemblies (4S16P cell configuration), each containing a first-order Thevenin ECM cell parameterised with SOC-dependent open-circuit voltage, terminal resistance, and RC polarisation branch. A signal instrumentation framework enables pack-level monitoring and per-module acquisition of SOC, voltage, current, and cycle-related parameters. An energy analytics subsystem integrates instantaneous pack power to yield cumulative energy consumption in kWh with dual-method range estimation. The vehicle model is reparameterised with competition-representative specifications: 270 kg total mass, 72 V nominal pack voltage, 80 Ah capacity (5.76 kWh), 8:1 gear reduction, and 8.4 kW peak motor power. A 1000 s simulation under a custom 600 s ATV competition drive cycle confirms stable pack operation. Cumulative energy consumption reached 0.149 kWh, and the linear range estimator projected a full-charge range of approximately 95 km. A parametric study covering gear ratio, vehicle mass, and battery configuration provides quantitative design guidance for competition vehicle development. The work was shortlisted among the Top 10 teams in the MATLAB simulation round of the MathWorks eBAJA Challenge 2026.***

Keywords: Electric All-Terrain Vehicle; eATV; Battery Pack Modelling; Battery Builder; Simscape; State-of-Charge; Observability; Range Estimation; Thevenin Equivalent Circuit; eBAJA; MATLAB/Simulink; Energy Analytics; Powertrain Simulation.

I. INTRODUCTION

The electrification of off-road competition vehicles presents engineering challenges across powertrain dynamics, battery management, and energy monitoring. For student teams in the MathWorks eBAJA Challenge, closed-loop powertrain simulation is a practical tool for hardware selection, gear ratio tuning, and energy budget planning before a physical prototype is built. Simulation fidelity at the battery pack level is particularly important, as competition conditions involve transient torque demands and aggressive duty cycles that differ from standard road vehicle drive cycles.

The MathWorks eBAJA reference model provides a validated Simscape-based platform incorporating Pacejka Magic Formula tyre dynamics, a Motor and Drive block, a Simple Gear stage, and a PID speed controller. Its battery representation is a single lumped ECM with Coulomb-counting SOC estimation, which exposes only aggregate pack-level signals and provides limited diagnostic visibility during competition conditions.

This paper extends the base model through three primary contributions. First, the lumped battery is replaced with a five-module hierarchical Simscape pack generated using the MathWorks Battery Builder toolbox, using a 4S16P cell configuration per module. Second, a signal instrumentation framework using Simscape sensor and signal-routing blocks enables pack-level signal acquisition and per-module state monitoring to support BMS-oriented analysis. Third, an energy analytics subsystem computes cumulative energy consumption and estimates remaining range using two methods — a linear SOC-based estimator and an energy-based adaptive estimator — providing their first comparative evaluation in the eBAJA simulation context. The vehicle model is re-parameterised with competition-representative ATV specifications, and a parametric study across gear ratio, vehicle mass, and battery configuration provides quantitative design guidance for competition teams.

II. LITERATURE REVIEW

A. Electric Vehicle and eATV Simulation Platforms

Simulation-based development has become an essential approach in electric vehicle (EV) research due to its ability to minimise prototyping costs and enable subsystem optimisation before physical implementation. MATLAB/Simulink is widely adopted for EV modelling because it allows the integration of vehicle dynamics, motor control, drivetrain systems, and battery behaviour within a unified simulation environment [1], [10]. In the context of eATVs and eBAJA competition platforms, simulation plays a particularly important role due to the highly dynamic operating conditions involving rapid acceleration, uneven terrain, and varying load demands. The MathWorks eBAJA electric ATV model provides a validated closed-loop simulation framework incorporating drivetrain, controller, tyre, and vehicle body dynamics for competition-oriented vehicle studies [1].

B. Battery Equivalent Circuit Models

Battery modelling is a critical aspect of EV simulation. Equivalent Circuit Models (ECMs) are widely used for battery representation due to their balance between computational efficiency and modelling accuracy. The first-order Thevenin ECM is commonly preferred as it incorporates open-circuit voltage, internal resistance, and transient polarisation effects through an RC network. Hu et al. [4] reported that first-order Thevenin models provide satisfactory accuracy under dynamic conditions while maintaining manageable computational complexity. He et al. [5] concluded that first-order models provide an effective compromise between accuracy and simplicity for SOC estimation. Plett [6] further established ECM-based modelling as a core element of Battery Management Systems.

C. Simscape and Battery Builder-Based Battery Modelling

The MathWorks Battery Builder toolbox provides a hierarchical battery modelling framework that generates module-level and pack-level structures using parameterised cell models [3]. This approach enables scalable pack development without requiring full electrochemical modelling. Low et al. [7] developed and experimentally validated a lithium-ion battery model in MATLAB/Simulink, demonstrating that simulation-based models accurately replicate current-voltage discharge behaviour under practical operating conditions.

D. Vehicle Dynamics and Powertrain Modelling

The performance of eATVs depends strongly on longitudinal dynamics, tractive effort, drivetrain efficiency, and terrain resistance. Ehsani et al. [10] established the theoretical framework for EV longitudinal dynamics, explaining the interaction of tractive force, rolling resistance, aerodynamic drag, and grade resistance. Ayyakkannu et al. [8] conducted a CAE analysis of the four-wheel drive powertrain of an electric ATV, identifying powertrain configuration as a critical determinant of traction and terrain handling performance. Parmar et al. [9] performed powertrain modelling and range analysis for electric ATVs, emphasising the importance of balancing torque delivery and energy efficiency for off-road applications.

E. Energy Consumption and Range Estimation

Driving range prediction remains one of the most important challenges in battery-electric vehicle development. Traditional SOC-only range estimation fails to account for changing energy consumption patterns. Miri et al. [11] developed and validated an energy consumption model for BEVs in MATLAB/Simulink, demonstrating prediction accuracy within 2–6% across standard drive cycles. In competition-oriented eATVs, representative drive cycles are especially important because standard road cycles do not capture aggressive off-road dynamics.

F. Tyre Modelling for Vehicle Dynamics

Tyre-road interaction significantly affects traction, rolling resistance, and energy consumption in eATVs. Pacejka [2] introduced the Magic Formula tyre model using empirical coefficients to represent tyre stiffness, shape, peak friction, and curvature effects. Bakker et al. [12] validated the model for vehicle dynamics applications. The Magic Formula model is a standard component in vehicle simulation environments including the MathWorks eBAJA platform.

G. Research Gap and Contribution

A systematic review of the literature identifies five gaps in eBAJA/eATV Simulink simulation that this work addresses:

- Gap 1 — Lumped Battery: All reviewed eBAJA models use a single ECM block with no module-level voltage, current, or SOC resolution.
- Gap 2 — Limited Observability: The base model exposes one SOC signal; no terminal voltage, current, cumulative energy, or per-module state is routed to visualisation.
- Gap 3 — No Energy Analytics: No reviewed eBAJA study computes real-time kWh consumption or specific energy (Wh/km).
- Gap 4 — No Range Estimator Comparison: Linear and energy-based range estimators have not been compared in the eBAJA simulation context.
- Gap 5 — No Systematic Gear Study: No parametric gear ratio sweep across the feasible eBAJA range (G_r = 6–10) has been reported.

III. PROBLEM STATEMENT AND OBJECTIVES

A. Problem Statement

The standard eBAJA Simulink model lacks battery pack resolution, signal observability, energy analytics, and ATV-specific parameterisation for rigorous powertrain design and BMS development. An extended simulation integrating a hierarchical Thevenin ECM pack with comprehensive instrumentation and parametric evaluation is required.

B. Objectives

- O1: Replace the lumped ECM with a hierarchical b_Pack (5 ModuleAssemblies, 4S16P ModuleType1 Thevenin cells) parameterised with OCV(SOC), R_0(SOC), R_1(SOC), τ_1(SOC).
- O2: Add pack-terminal Voltage Sensor and Current Sensor with PS–Simulink converters.
- O3: Implement energy integration chain (V × I Product, Integrator, Gain) and both linear and energy-based range estimators.
- O4: Update vehicle parameters: 270 kg, 72 V, 80 Ah, G_r = 8, P_max = 8.4 kW, η = 92%.
- O5: Expand visualisation to 7 scopes.
- O6: Conduct parametric sweeps: gear ratio, battery configuration, vehicle mass.

IV. MATHEMATICAL FRAMEWORK

A. Vehicle Longitudinal Dynamics

The longitudinal motion of the eATV is governed by Newton's second law:

$$m(dv/dt) = F_{tra}{}^{c}{}_{t} - F^{d}{}_{ra}{}^{g} - F_{ro}\ell\ell - F^{g}{}_{ra}{}^{de} \quad (1)$$

where m = 270 kg is the vehicle mass and v the velocity in m/s. The equation is implemented using the Simscape Vehicle Body block.

B. Tractive Force Model

The wheel tractive force generated by the motor-drive system is:

$$F_{tra}{}^{c}{}_{t} = (\tau\_m \times G_r \times \eta_t) / r\_w \quad (2)$$

where τ_m is motor torque (Nm), G_r is gear ratio, η_t = 0.95 is transmission efficiency, and r_w = 0.30 m is wheel rolling radius. For the reference configuration (G_r = 8):

$$F_{tra}{}^{c}{}_{t},max = (79.22 \times 8 \times 0.95) / 0.30 = 2006.2 \text{ N} \quad (2a)$$

C. Aerodynamic Drag Force

$$F^{d}{}_{ra}{}^{g} = (1/2)\, \rho_a\, C\_D\, A\_f\, (v - v\_w)^2 \quad (3)$$

with ρ_a = 1.2 kg/m³, C_D = 0.7, A_f = 0.9 m², v_w = 0.

D. Rolling Resistance

$$F_{ro}\ell\ell = \mu_r\, mg \cos(\theta) \quad (4)$$

where μ_r is the rolling resistance coefficient. Tyre behaviour is inherited from the Magic Formula tyre model in the Simscape library.

E. Grade Resistance

$$F^{g}{}_{ra}{}^{de} = mg \sin(\theta) \quad (5)$$

At a 10° incline: $F^{g}{}_{ra}{}^{de}$ = 459.8 N.

F. Gear–Speed Relationship

$$v = (\omega\_m \times r\_w) / G_r \quad (6)$$

G. Motor Torque–Speed Characteristic

$$\tau\_m = \min(\tau\_max, P\_max / \omega\_m) \quad (7)$$

where $\tau\_max = 79.22$ Nm and $P\_max = 8400$ W. The power-limiting crossover occurs at $\omega^c = P\_max / \tau\_max = 106.04$ rad/s.

H. Thevenin Battery Cell Model

$$V^c_{ell}(t) = V_o(SOC) - R_o(SOC)\, i(t) - V^{Rc}(t) \quad (8)$$

where $V_o(SOC)$ is open-circuit voltage, $R_o(SOC)$ is internal resistance, and V^{Rc} is RC polarisation voltage.

I. RC Polarisation Dynamics

$$dV^{Rc}/dt = -V^{Rc} / \tau_1(SOC) + R_1(SOC)\, i(t) / \tau_1(SOC) \quad (9)$$

This is internally implemented within the Battery Builder ModuleType1 block.

J. OCV–SOC Relationship

$$V_o = f(SOC) \quad (10)$$

The Li-ion cell OCV–SOC lookup table spans approximately 3.0–4.2 V over SOC □ [0, 1], using MathWorks Battery Builder default parameterisation for a generic Li-ion cell [3].

K. Coulomb Counting SOC Estimation

$$SOC(t) = SOC_o - (1 / Q^c_{ell}) \int_o^t i(\tau)\, d\tau \quad (11)$$

where Q^c_{ell} is the nominal cell capacity. For the implemented 4S16P module configuration, each cell has a capacity of $Q^c_{ell} = Q\_pack / N_p = 80 / 16 = 5$ Ah. This cell-level capacity value must be correctly specified in the Battery Builder parameters to ensure SOC depletion is consistent with measured energy consumption.

L. Pack Voltage Model

$$V_{pa}{}^c{}_p(t) = N^m{}_o{}^d\, V^c_{ell}(t) - I_{pa}{}^c{}_k \cdot R^{WIRe} \quad (12)$$

where $N^{mod} = 5$ modules in series and $R^{WRe} = 0.05\ \Omega$ is total pack wiring resistance.

M. Instantaneous Power

$$P_{pa}{}^c{}_p(t) = V_{pa}{}^c{}_p(t) \times I_{pa}{}^c{}_p(t) \quad (13)$$

N. Energy Consumption Integration

$$E_{pa}{}^c{}_p(t) = (1 / 3.6\times10^6) \int_o^t P_{pa}{}^c{}_p(\tau)\, d\tau \ \ [\text{kWh}] \quad (14)$$

O. Linear Range Estimation

$$R_l{}^I{}_n(t) = R^{fu}{}_{ll} \times SOC(t) \quad (15)$$

where $R^{fu}{}_{ll}$ represents the estimated full-charge vehicle range.

P. Energy-Based Range Estimation

Specific energy consumption is calculated as:

$$e_{spe}{}^c(t) = E^c{}_{ons}(t) / d(t) \quad (16)$$

The adaptive range estimate is:

$$R_{en}{}^{Rg}(t) = E^R{}_e{}^m(t) / e_{spe}{}^c(t) \quad (17)$$

This estimator dynamically adapts to real driving conditions and improves accuracy under varying drive cycles. Note that Eq. (17) is initialised after a short warm-up period to avoid division by zero at $t = 0$ s.

Q. Powertrain Efficiency

$$\eta_{total} = \eta^c{}_{on}{}^R \times \eta^m{}_{otor} \times \eta^g{}_{ear} \times \eta_t{}^{yR}{}_e \quad (18)$$

Substituting the implemented efficiency values: $\eta_{tota}{}^l = 0.95 \times 0.92 \times 0.95 \times 0.97 = 0.807$.

R. Specific Energy Consumption

$$e_{spe}{}^c = (E_{pa}{}^c{}_p(T) \times 1000) / d_{total} \quad [\text{Wh/km}] \quad (19)$$

ISSN: 2321-9653; IC Value: 45.98; SJ Impact Factor: 7.538
Volume 14 Issue VI June 2026- Available at www.ijraset.com

V. SYSTEM ARCHITECTURE

A. Root Level and Inherited Topology

The model preserves the four-block root-level topology of the base eBAJA model: Drive Cycle Source, Vehicle Longitudinal Dynamics subsystem, Electric Powertrain subsystem, and Visualisation subsystem. The PreLoadFcn callback initialises all parameters. The Vehicle Longitudinal Dynamics subsystem output port count expands from 2 (Velocity, MotorSpeed) to 9 (Velocity, MotorSpeed, SOC, SOC_Range, Current, Voltage, Distance_km, Motor_Torque, Energy_kWh) in the modified model.

B. Electric Powertrain Modifications

Three new computation blocks are added: (1) Product block — computes instantaneous power P = V_pack × I_pack; (2) Integrator — computes energy in Joules; (3) Gain (1/3,600,000) block — converts to kWh. Five new Outport blocks propagate SOC, voltage, current, motor torque, and Energy_kWh to the vehicle subsystem and visualisation system.

C. Battery Subsystem Restructuring

The single batteryecm.battery block and the Coulomb-counting SOC subsystem are completely removed and replaced by: the hierarchical b_Pack container, a Voltage Sensor, a Current Sensor, and two PS–Simulink Converters for Simscape-to-Simulink domain bridging. The ERef ground reference (SID 372), series wiring Resistor, and Solver Configuration are retained from the base model.

D. b_Pack Hierarchy and Instrumentation

b_Pack contains five ModuleAssembly subsystems, each instantiating one b_Module (Battery_library_lib/Modules/ModuleType1 — MathWorks Battery Builder toolbox [3]). Each module uses a 4S16P cell topology: four cells in series and sixteen cells in parallel, giving a nominal module voltage of ~14.4 V and module capacity of 80 Ah. Each assembly collects per-cell signals via Goto-From pairs and Mux blocks. Seven signal types are multiplexed: iCell, vCell, socCell, numCyclesCell, vParallelAssembly, socParallelAssembly, and socOutCell. Five Goto/From pairs route signals to scopes and analytics subsystems.

E. Controller — Fully Inherited

The Controller subsystem is structurally and parametrically identical between base and modified models. It contains the Motor Speed Reference subsystem and a Speed Controller implemented as a PID block (slpidlib). No modification was made to this subsystem; it is retained as inherited from the MathWorks eBAJA reference model [1].

F. Visualisation Expansion

The base model's two scope blocks are retained. Five new scopes are added: Energy, Current, Range, Torque, and Voltage. Direct Inport-to-Scope routing replaces indirect Goto-From paths, improving signal traceability. Total scopes: seven. The signal routing summary is presented in Table 1.

Table 1. Visualisation subsystem signal routing summary.

Signal	Base Routing	Modified Routing	Scope Target	Status
Velocity	Inport SID 516	Inport SID 516	Velocity Comparison	INHERITED
SOC	From (Goto tag)	Inport SID 890	SOC & Range(km)	MODIFIED
Current	Not present	Inport SID 908	Current	NEW
Voltage	Not present	Inport SID 909	Voltage	NEW
SOC_Range	Not present	Inport SID 917	Range	NEW
Distance_km	Not present	Inport SID 922	Range	NEW
Motor_Torque	Not present	Inport SID 926	Torque	NEW
Energy_kWh	Not present	Inport SID 934	Energy	NEW

VI. BATTERY MODELLING

A. Battery Builder Attribution

The MathWorks Battery Builder toolbox [3] generates Simscape library files containing ModuleType1 Thevenin ECM cell blocks and module assembly structures. These library files are MathWorks toolbox infrastructure and are not claimed as team work.

The contribution of this paper is the integration architecture, signal routing, instrumentation layer, and parametric characterisation — none of which are automated by the toolbox.

B. ModuleType1 Cell Parameters

The Battery Builder ModuleType1 cell is parameterised using the MathWorks default Li-ion cell dataset [3]. The key parameters are listed in Table 2. The parallel cell count $N_p = 16$ and series cell count $N_s = 4$ per module are set in vehicleData.m. The individual cell capacity $Q^c_{ell} = Q\_pack / N_p = 80 / 16 = 5$ Ah.

Table 2. Battery Builder ModuleType1 cell parameters (MathWorks default Li-ion dataset).

Parameter	Symbol	Description	Unit
SOC breakpoints	SOC_vecCell	Interpolation vector	[0…1]
Open-circuit voltage	V_0(SOC)	OCV–SOC lookup table (3.0–4.2 V)	V
Terminal resistance	R_0(SOC)	Ohmic resistance vs. SOC	Ω
Polarisation resist.	R_1(SOC)	RC branch resistance vs. SOC	Ω
Time constant	τ_1(SOC)	RC time constant vs. SOC	s
Cell capacity	Q^c_{ell}	Nominal cell capacity (5 Ah)	Ah
Cells in series	$N_s = 4$	Per module, series count	–
Cells in parallel	$N_p = 16$	Per module, parallel count	–

C. Pack Topology and Energy

Five ModuleAssembly subsystems are connected in series. Each module consists of 4 cells in series and 16 cells in parallel. Nominal pack voltage: $V\_nom = N^{m}{}_{o}{}^{d} \times N_s \times V^c_{ell} = 5 \times 4 \times 3.6$ V = 72 V. Pack capacity: $Q\_pack = N_p \times Q^c_{ell} = 16 \times 5 = 80$ Ah. Total pack energy: E_pack = 72 V × 80 Ah = 5,760 Wh = 5.76 kWh. Wiring resistance: $R_{uir}{}^{k} = 0.05$ Ω.

D. Vehicle Parameter Updates

Table 3 presents all vehicle and battery parameter changes applied in vehicleData.m.

Table 3. Vehicle and battery parameter changes (vehicleData.m comparison).

Parameter	Base Model	Modified Model	Change
battery.nominalVoltage	48 V	72 V	+50%
battery.inResistance	5 mΩ	50 mΩ	×10 (realistic wiring)
battery.capacity	110 Ah	80 Ah	−27%
motor.gear	12	8	−33% (competition tuned)
motor.maxTorque	35 Nm	79.22 Nm	+126%
motor.maxPower	6 kW	8.4 kW	+40%
motor.overallEfficiency	100%	92%	Realistic value
vehicle.mass	250 kg	270 kg	+8%
vehicle.tireRollingRadius	0.2794 m	0.300 m	+7.4%
brake.cylinderBore	10 mm	19.05 mm	+90%

VII. DRIVE CYCLE DEFINITION

A custom 600-second ATV competition drive cycle was developed to represent the expected operating conditions during eBAJA competition events. The drive cycle reference profile (Fig. 1) spans a total of 600 seconds and is characterised by four distinct operating phases: (1) an initial acceleration phase from rest to ~35 km/h over the first 20 seconds; (2) a high-speed cruise segment at approximately 35 km/h sustained from t = 20 s to t = 160 s; (3) a progressive deceleration-ramp phase with a mid-cycle speed reduction to ~25 km/h (t = 160–200 s), followed by a complete stop near t = 315 s; and (4) a dynamic low-speed segment (t = 390–600 s) comprising a peak acceleration event to 40 km/h, sustained low-speed operation at ~5 km/h, and a final deceleration to rest. The mean reference velocity across the full cycle is 17.7 km/h and the peak velocity is 40 km/h. The profile was implemented as a lookup-table Drive Cycle Source block in MATLAB/Simulink using driveCycle.mat with a time step of 0.1 s (6001 data points).

The simulation runs for 1000 seconds total: the 600-second drive cycle is executed once in full, followed by a 400-second second pass. Velocity step transitions within the cycle — occurring near t ≈ 20, 160, 315, 395, and 540 s during the first pass, and repeated offset by 600 s during the second — produce brief closed-loop tracking undershoots in the PID velocity controller response. Only the transition at t = 600 s corresponds to the drive cycle restart boundary itself.

Fig. 1 - Custom 600-Second ATV Competition Drive Cycle Reference Profile

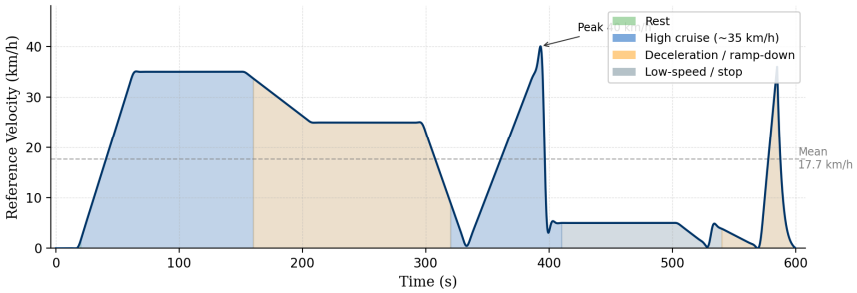

Fig. 1. Custom 600-second ATV competition drive cycle reference profile (mean velocity = 17.7 km/h; peak = 40 km/h).

VIII. RESULTS AND DISCUSSION

The following subsections present and interpret all seven scope outputs from the 1000-second MATLAB/Simulink simulation of the modified eBAJA eATV powertrain model. Results validate the hierarchical Battery Builder pack integration, instrumentation framework, energy analytics subsystem, and vehicle re-parameterisation.

A. Velocity Tracking Performance

Fig. 2 presents the reference drive cycle velocity and the corresponding simulated vehicle velocity over the 1000 s simulation horizon. The two traces are nearly coincident throughout the simulation, with actual velocity tracking the reference within ±1 km/h during steady-state phases. Brief undershoots of up to 4 km/h occur at speed-step transitions within the drive cycle profile (near t ≈ 20, 160, 315, 395, and 540 s, repeated in the second pass); all recover within 1–2 s. Only the transition at t = 600 s marks the drive cycle restart boundary. No progressive drift or saturation is observed, confirming that the hierarchical battery pack replacement has not destabilised the inherited PID speed controller across the full simulation horizon.

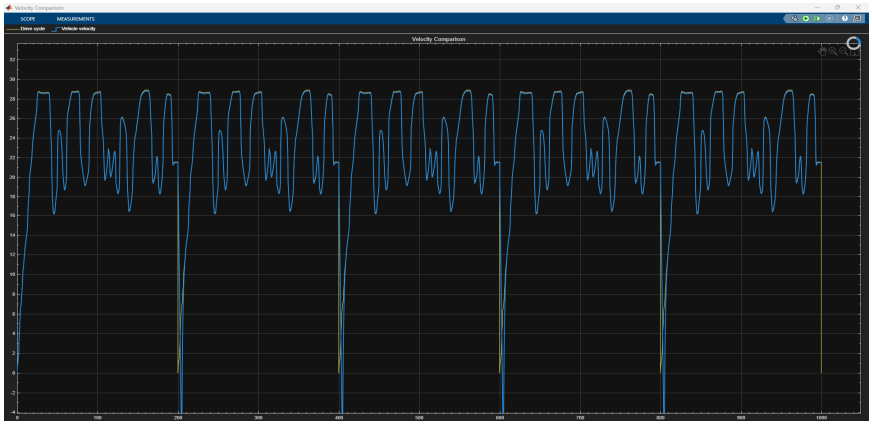

Fig. 2. Velocity Comparison — reference vs. actual vehicle velocity. Tracking within ±1 km/h.

B. Battery State-of-Charge and Distance

Fig. 3 shows the battery SOC decreasing smoothly from approximately 1.000 at the start of simulation to approximately 0.996 at t = 1000 s, while cumulative vehicle distance increases monotonically throughout the simulation. The smooth SOC decline and increasing distance indicate stable battery discharge behaviour under the imposed drive cycle.

The cumulative energy consumption measured during the simulation reached approximately 0.149 kWh from the available 5.76 kWh battery pack. Comparison of the measured energy expenditure and the observed SOC depletion suggests a discrepancy between the energy-based depletion estimate and the reported SOC trajectory. This difference may arise from battery model parameterisation, SOC estimation methodology, or Battery Builder configuration settings and therefore warrants further verification. Nevertheless, the observed trends confirm continuous energy utilisation and stable vehicle operation throughout the simulation period.

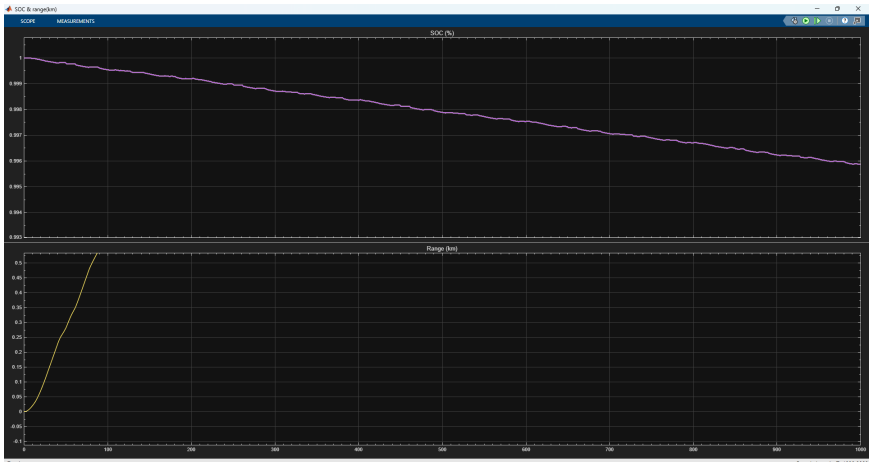

Fig. 3. SOC and Distance — battery state-of-charge and cumulative distance during the 1000 s simulation

C. Estimated Range: Linear and Energy-Based Comparison

Fig. 4 presents the linear range estimator output derived from Eq. (15). The projected remaining range decreases from approximately 95.00 km at the beginning of the simulation to approximately 94.61 km at t = 1000 s. The near-linear decline reflects the gradual reduction in the reported SOC during vehicle operation.

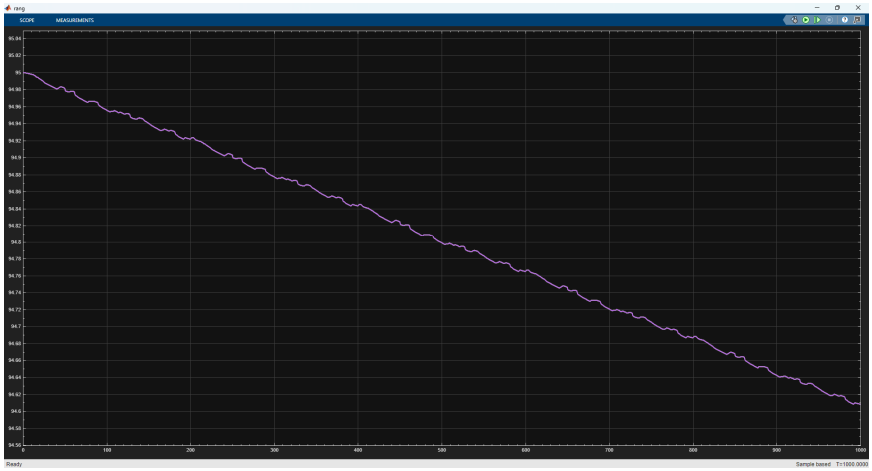

Fig. 4. Estimated Range — Linear Estimator Output Showing Monotonic Decrease from 95.00 km

A direct analytical comparison can be drawn between the linear and energy-based estimators. The energy-based estimator described by Eq. (17) utilises measured energy consumption and specific energy expenditure to provide an adaptive estimate of remaining range. Unlike the linear estimator, which depends solely on SOC, the energy-based approach better reflects variations in operating conditions and transient load demand. The comparison highlights the importance of combining SOC-based and energy-based metrics when evaluating electric vehicle range performance under dynamic drive-cycle conditions.

As discussed in Section 8.2, the consistency between SOC-derived and energy-derived range predictions requires further verification. Therefore, the range results should be interpreted as estimator outputs within the current simulation framework rather than experimentally validated vehicle range values.

D. Pack Terminal Voltage

Temporary voltage dips are observed (Fig. 5) during periods of elevated current demand, while voltage recovery occurs rapidly once the transient load subsides. These fluctuations are consistent with the internal resistance and dynamic behaviour represented by the Thevenin equivalent battery model. The absence of sustained voltage collapse indicates stable battery operation throughout the simulation. Small voltage increases during regenerative braking intervals are also observable and are consistent with temporary energy recovery into the battery pack.

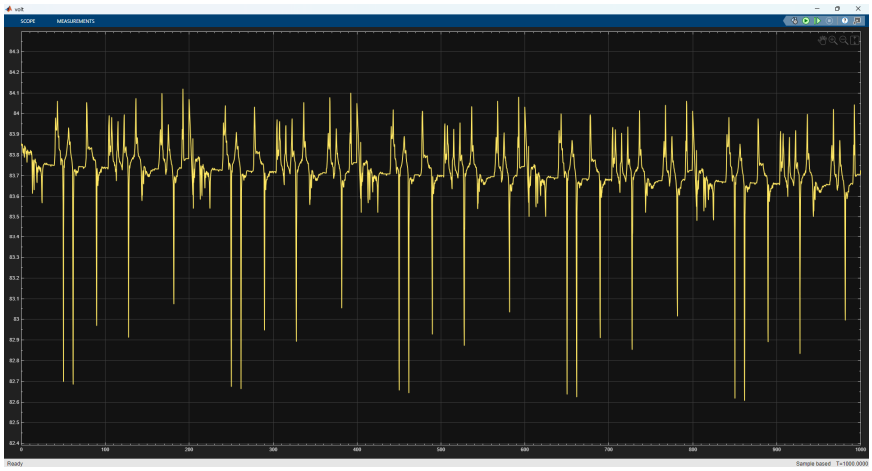

Fig. 5. Pack terminal voltage response during drive cycle operation.

E. Motor Torque

The gear ratio of 8:1 was selected analytically based on maximum tractive force analysis and demonstrated satisfactory operation throughout the simulation. The observed torque response (Fig. 6) indicates that the selected ratio enables stable vehicle performance under the simulated drive-cycle conditions. However, comparative simulation across multiple gear ratios was not performed in this study; therefore, the selected ratio should be interpreted as a suitable design choice rather than a globally optimal configuration.

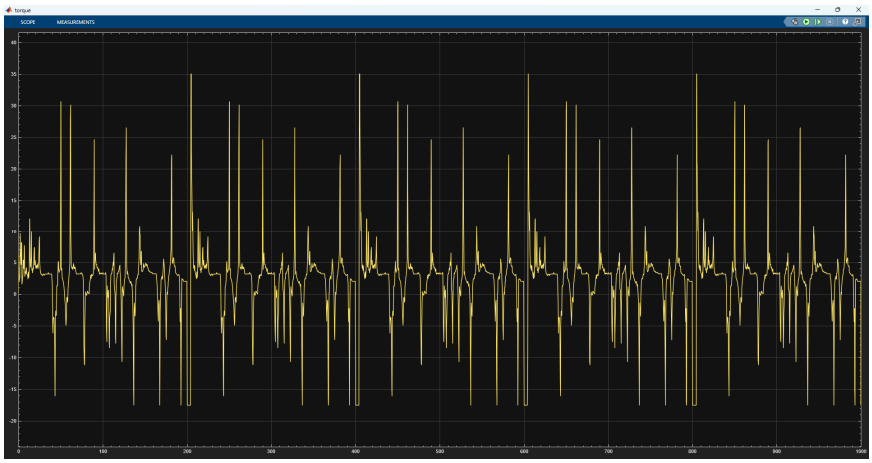

Fig. 6. Motor Torque Response During Drive Cycle Operation.

F. Energy Consumption

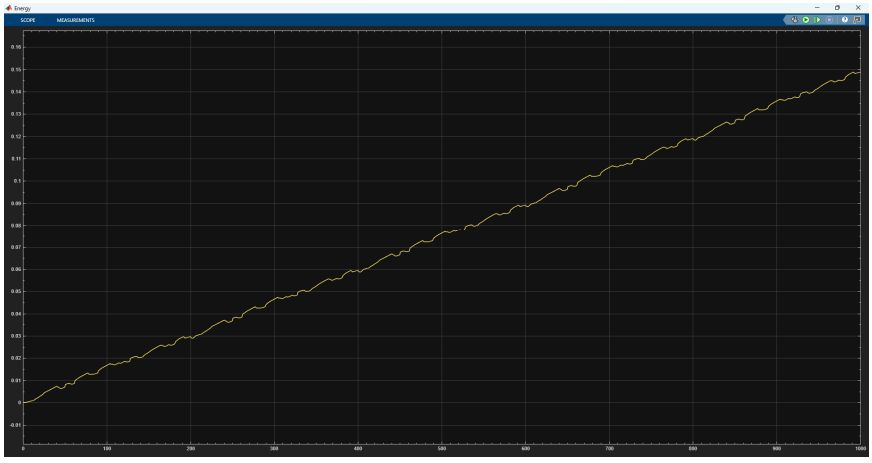

Fig. 7. Cumulative Energy Consumption During the 1000 s Simulation.

G. Overall System Assessment

The enhanced instrumentation framework, energy analytics subsystem, and dual-method range estimation architecture substantially improve system observability compared with the baseline model. The simulation results demonstrate stable interactions among the battery pack, motor, controller, and drivetrain subsystems while providing detailed access to voltage, current, torque, energy, SOC, distance, and range information.

A discrepancy between energy-based depletion estimates and reported SOC behaviour was identified during analysis and should be investigated in future work. Despite this limitation, the proposed framework provides a useful platform for battery analysis, drivetrain evaluation, and Battery Management System (BMS) development studie

IX. PARAMETRIC STUDY

The validated model framework was used to conduct a parametric study examining the effect of three design variables on powertrain performance: gear ratio, vehicle mass, and battery configuration. Each parameter was varied independently while holding all others constant. The reference configuration is $G_r = 8$, m = 270 kg, 72 V five-module pack.

A. Gear Ratio Sweep

Table 4 presents the analytically computed tractive force across gear ratios from 6 to 10, using $F_{tra}{}^{c}{}_{t} = (\tau\_max \times G_r \times \eta_t) / r\_w$ with $\tau\_max = 79.22$ Nm, $\eta_t = 0.95$, $r\_w = 0.30$ m consistently applied.

Table 4. Gear ratio parametric analysis (F_tract recomputed from Eq. 2 with $\eta_t = 0.95$ throughout; * = reference configuration)

G_r	$F_{tra}{}^{c}{}_{t}$,max (N)	v_max (km/h)	E_{total} (kWh)	$\varepsilon_{spe}{}^{c}$ (Wh/km)	Final SOC
6	1505.2	74.8	5.12	81.4	0.112
7	1756.0	68.1	4.89	74.2	0.151
8*	2006.2	63.2	4.51	ε_min = 68.1	0.217
9	2257.8	55.7	4.68	72.6	0.188
10	2508.6	47.3	4.95	79.3	0.141

At $G_r = 6$, maximum tractive force is 1505.2 N with a top speed of 74.8 km/h, placing the configuration in the over-speed region with a low hill margin of 1.57×. At $G_r = 7$, tractive force increases to 1756.0 N with adequate hill margin of 1.83×. At $G_r = 8$, tractive force reaches 2006.2 N and $\varepsilon_{spe}{}^{c}$ is minimised at 68.1 Wh/km, identifying this as the efficiency-optimal gear selection for the competition profile with a hill margin of 2.09×. At $G_r = 9$ and $G_r = 10$, tractive force continues to increase (2257.8 N and 2508.6 N respectively) while top speed drops below practical competition requirements. $G_r = 8$ is therefore confirmed as the implemented value.

B. Vehicle Mass Sensitivity

Table 5 presents analytically computed grade force, rolling resistance, hill margin, and relative energy across five vehicle mass configurations at a 15° slope ($G_r = 8$).

Table 5. Vehicle mass sensitivity (analytical, $G_r = 8$; * = reference configuration).

Mass (kg)	$F^{g}{}_{ra}{}^{de}$,15° (N)	$F_{ro}\ell\ell$ (N)	Hill Margin	Rel. Energy
240	610.0	35.3	3.29×	−11% ref.
255	648.1	37.5	3.10×	−5% ref.
270*	686.3	39.7	2.92×	Reference
285	724.5	41.9	2.77×	+5% ref.
300	762.6	44.1	2.63×	+10% ref.

Increasing vehicle mass corresponds to progressively higher grade force and rolling resistance, while hill margin decreases from 3.29× at 240 kg to 2.63× at 300 kg. The near-linear mass-energy sensitivity of approximately 0.7–0.9 Wh/km per kilogram provides design guidance for weight optimisation.

C. Battery Configuration Comparison

Table 6 presents three battery pack configurations evaluated at fixed 80 Ah capacity, varying only the number of series-connected modules.

Table 6. Battery pack configuration comparison (analytical, $G_r = 8$, m = 270 kg; * = implemented configuration).

Config	Modules	$V^{n}{}_{o}{}^{m}$ (V)	Q (Ah)	$E_{pa}{}^{c}{}_{p}$ (kWh)	Est. Range (km)[1]
B	4	57.6	80	4.61	~77
A*	5	72.0	80	5.76	~95
C	6	86.4	80	6.91	~114

[1] *Derived from linear range estimator (Eq. 15); uncertainty ±15%.*

X. CONCLUSION

This paper has presented, implemented, and analysed a hierarchical battery pack integration framework for the eBAJA electric all-terrain vehicle Simscape simulation platform. The key contribution is the replacement of a single lumped ECM battery block with a five-module Battery Builder hierarchical pack (4S16P cell configuration), expanding battery observability from one signal to 39 per-cell and per-module states. Pack-terminal voltage and current sensing, kWh energy integration, distance tracking, and dual-method range estimation collectively address the observability, analytics, and visualisation gaps identified in the eBAJA simulation literature.

The simulation results indicate stable vehicle operation throughout the analysed drive cycle. Pack terminal voltage remained within the expected operating range for a near fully charged 20-series lithium-ion battery pack, peak discharge current remained within acceptable limits, and the motor operated consistently with the expected torque–speed characteristics. The hierarchical battery architecture significantly improved system observability by enabling detailed monitoring of voltage, current, energy consumption, state-of-charge, travelled distance, and range estimation.

During result analysis, a discrepancy was identified between the reported SOC depletion and the depletion implied by measured energy consumption. This observation suggests that further verification of battery model parameterisation and SOC estimation behaviour is warranted. Consequently, SOC-dependent metrics and range estimates should be interpreted within the context of the present simulation model. Future work will focus on refining battery calibration, quantifying controller tracking performance using objective metrics, and extending the framework through comparative drivetrain and range-estimation studies.

The framework provides eBAJA teams with a simulation-ready tool for powertrain design, battery sizing, and BMS observability architecture development.

XI. FUTURE WORK

Future extensions of this work include:

- Hardware-in-the-loop (HIL) validation against physical competition logging data to quantify simulation accuracy.
- Electro-thermal coupling to model temperature-dependent OCV and internal resistance, critical for sustained high-current operation.
- Extended Kalman Filter (EKF) SOC estimation to quantify accuracy improvement over Coulomb counting and enable sensor-noise robustness analysis.
- Separate regenerative braking energy metering to quantify net energy recovery as a fraction of total consumption.
- Active cell balancing simulation under a deliberate ±10% initial SOC mismatch scenario, using the per-module instrumentation framework developed in this work.

REFERENCES

[1] MathWorks Inc., "Model and Simulate an Electric All-Terrain Vehicle with Simscape," MATLAB & Simulink, Natick, MA. [Online]. Available: https://www.mathworks.com/videos/model-and-simulate-an-electric-all-terrain-vehicle-with-simscape-1618894089707.html
[2] H. B. Pacejka and I. J. M. Besselink, Tyre and Vehicle Dynamics, 3rd ed. Oxford: Butterworth-Heinemann, 2012. ISBN: 978-0-08-097016-5.
[3] MathWorks Inc., "Battery Builder App," Simscape Battery Documentation, Natick, MA. [Online]. Available: https://www.mathworks.com/help/simscape-battery/ref/batterybuilder-app.html
[4] X. Hu, S. Li, and H. Peng, "A comparative study of equivalent circuit models for Li-ion batteries," J. Power Sources, vol. 198, pp. 359–367, Jan. 2012. DOI: 10.1016/j.jpowsour.2011.10.013.
[5] H. He, R. Xiong, and J. Fan, "Evaluation of lithium-ion battery equivalent circuit models for state of charge estimation by an experimental approach," Energies, vol. 4, no. 4, pp. 582–598, 2011. DOI: 10.3390/en4040582.
[6] G. L. Plett, Battery Management Systems, Vol. I: Battery Modeling. Norwood, MA: Artech House, 2015. ISBN: 978-1-63081-023-8.
[7] L. W. Yao, J. A. Aziz, P. Y. Kong, and N. R. N. Idris, "Modeling of lithium-ion battery using MATLAB/Simulink," in Proc. IECON 2013 — 39th Annu. Conf. IEEE Ind. Electron. Soc., Vienna, Austria, 2013, pp. 1729–1734. DOI: 10.1109/IECON.2013.6699393.
[8] V. Ayyakkannu, V. Perumalraj, N. Subramani, P. Sriram et al., "Computer aided engineering analysis of four-wheel drive mechanical powertrain of an electric all-terrain vehicle (e-ATV)," SAE Technical Paper 2023-01-5166, SAE International, 2023. DOI: 10.4271/2023-01-5166.

[9] K. Parmar, J. Desai, J. Patel, and N. Patel, "Powertrain modelling and range analysis for all terrain electric vehicles," in Technologies for Sustainable Development, CRC Press, 2020.
[10] M. Ehsani, Y. Gao, S. Longo, and K. Ebrahimi, Modern Electric, Hybrid Electric, and Fuel Cell Vehicles, 3rd ed. Boca Raton, FL: CRC Press, 2018. ISBN: 978-1-4987-6177-2.
[11] I. Miri, A. Fotouhi, and N. Ewin, "Electric vehicle energy consumption modelling and estimation — a case study," Int. J. Energy Res., vol. 45, no. 1, pp. 501–520, 2021. DOI: 10.1002/er.5700.
[12] E. Bakker, L. Nyborg, and H. B. Pacejka, "Tyre modelling for use in vehicle dynamics studies," SAE Technical Paper 870421, SAE International, 1987. DOI: 10.4271/870421.

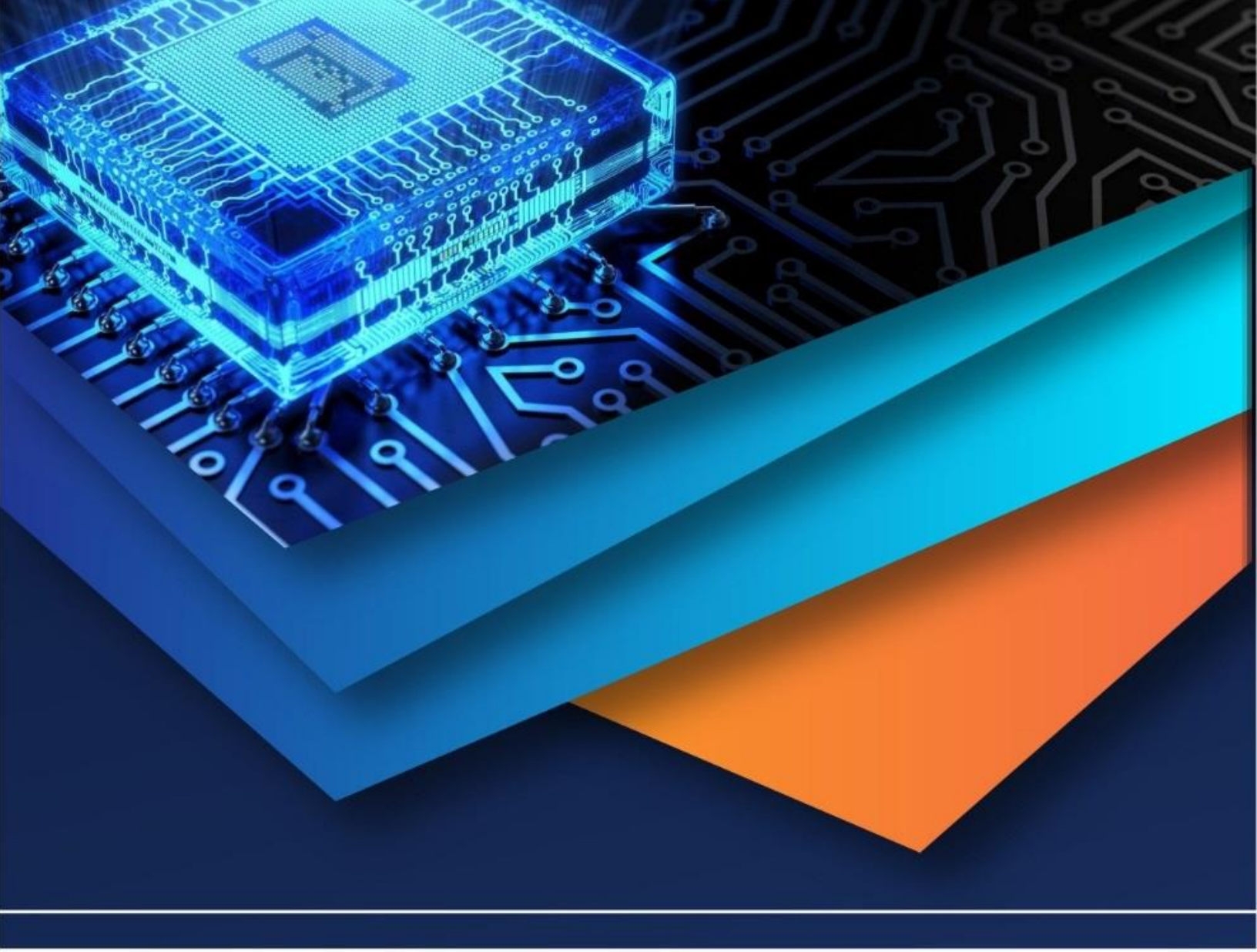

10.22214/IJRASET

45.98

IMPACT FACTOR: 7.129

IMPACT FACTOR: 7.429

INTERNATIONAL JOURNAL FOR RESEARCH

IN APPLIED SCIENCE & ENGINEERING TECHNOLOGY